ISSN No:-2456-2165

Experimental and Numerical Study on Fracture Behaviour of Steel and Basalt Fibre Reinforced Concrete Beams

Frajitha Franklin
M.Tech, Structural engineering
College of Engineering Trivandrum
Thiruvananthapuram, Kerala, India

Jayaprakash Jain K. G.
Associate professor
College of Engineering Trivandrum
Thiruvananthapuram, Kerala, India

Abstract:- Brittleness in concrete is one of the main disadvantage which increases with increase in the grade of concrete thereby increasing the formation of cracks. Fibres can be used to arrest the formation of cracks. Fracture mechanics is used in analysis of crack propagation in structures. In this study, notched beams were used to determine fracture parameters by conducting four point bending test. Beams with optimum percentage of basalt fibre, steel fibre and combination of basalt and steel fibre content respectively were used and fracture parameters were compared. Experimental results were used to validate the results obtained from numerical study using ABAQUS software. The fracture parameters like fracture energy, toughness, energy release rate, intrinsic brittleness and effective crack length increased with increase in percentage fibre content. Beams with basalt fibre content were found to have better fracture properties than beams with steel fibre content.

I. INTRODUCTION

➢ *General*

Concrete is the most widely used conventional material in the field of construction. Concrete has several advantaged which include its durability, formability and desired mechanical strength mainly compressive strength. Initially, the researchers focused on how to improve its compressive strength which is already one of its advantages. However its disadvantages include brittleness, low tensile strength, strain capacity, formation of cracks. Over the past few decades there has been a major evolution in the field of construction and new technologies, materials have been innovatively used to improve its strength. High strength concrete and ultra-high strength concrete are some of the examples which posses extremely higher compressive strength at early ages but also exhibit unusual brittleness.

Brittleness of concrete was found to increase with increase in grade of concrete. This in- turn increase the chances of formation of cracks. Once the crack is propagated, it leads to the failure of the structure. To overcome this disadvantage fibres are being used as an additive to the concrete. Fibres prevent the formation of crack by its bridging action and improve the ductility (Vikranth and Kavitha, 2012). Generally addition of fibres doesn't show much improvement in compressive strength. But the post-peak behavior of the stress–strain curve, compared to that of plain concrete (PC), is improved. Addition of fibres resist the formation of cracks by bridging crack face, fibres improve crack propagation and increases the energy absorption capacity of concrete. There are varieties of fibres used in the field of construction. The most commonly used fibre is steel fibre. But in past few years basalt fibre are being used to substitute steel fibres.

Steel fibres are materials which are cold drawn high strength wires, produced in steel making plants. These are available upto 60 mm length. The density of steel fibre is around 7850 kg/m^3 and the tensile strength is around 1100 MPa. These are available in the form of straight, hooked end, crimped, stranded and twisted. While basalt fibres are materials made from extremely fine fibres of basalt rock. It doesn't contain any additives which makes it more economical (Fathima, 2014). The density of basal fibre is around 2750 $kg/m^3$with tensile strength of 4840 MPa. These are available in the form of chopped fibres. Since the density of basalt fibre is lower, the amount of fibre used is lesser than steel fibre. Also the tensile strength is higher than steel fibre.

The concrete matrix consists of cracks and pore which cannot be eliminated. Hence the need to study the crack becomes important. Fracture mechanics deals with the study of the behavior of crack and its propagation in concrete. Concrete posses fracture behavior due to its heterogeneous nature and presence of fracture process zone. Presence of crack leads to stress concentration which in turn leads to growth of crack and finally causes failure of the structure.

This study mainly concentrates on the fracture behavior of steel fibre reinforced concrete (SFRC) and basalt fibre reinforced concrete (BFRC) and compares the behavior. The main aim is to compare both the fibres and to get an outcome of which among the fibres show better behavior.

II. EXPERIMENTALPROGRAMME

2.1 Materials and sample preparation

Ordinary Portland cement of 53 grade conforming to IS 12269:1970 was used. Laboratory tests were conducted to determine standard consistency and initial setting time, final setting time and compressive strength of mortar cubes at 7 and 28 days. The results conform to IS specifications.

ISSN No:-2456-2165

Sl. No.	Tests	Results
1	Standard consistency	34.6%
2	Initial setting time	150 minutes
3	Final setting time	380 minutes
4	7th day compressive strength	39.5 MPa
5	28th day compressive strength	54.4 MPa

Table 1:- Properties of cement

Aggregate of size 12m and 6 mm conforming to IS 383:1970 are used. M sand conforming to zone II was used as fine aggregates. The physical properties of coarse and fine aggregates as obtained through lab tests are given in table 2 and 3 respectively.

Sl. No.	Test Conducted	Result
1	Bulk density	1.598 g/cc
2	Specific gravity	2.67
3	Void ratio	0.66
4	Porosity	40%

Table 2:- Properties of coarse aggregate

Sl. No.	Test Conducted	Result
1	Bulk density	1.983 g/cc
2	Specific gravity	2.54
3	Void ratio	0.297
4	Porosity	21.8%

Table 3:- Properties of fine aggregate

Superplasticizers which is also known as high range water reducers, are chemical admixtures used for well dispersion of particle suspension. Superplasticizers are used to avoid particle segregation of gravel, coarse and fine sand, and to improve its flow the addition of superplasticizers in concrete mortar reduces the water cement ratio without affecting the workability of the mixture. Use of such admixture helps to generate self consolidating concrete and high strength concrete. It helps to improve the performance of hardened concrete. Since use of such admixtures helps to reduce water cement ratio it increases the strength properties of hardened concrete. The pH value of admixture used is 6 and volumetric mass of 1.09 kg/litre is used. It appears to be light yellow coloured with an alkali content of less than 1.5g.

Hooked end steel fibre of non-glued type is used in concrete. Properties of steel fibres provided by manufacturers are represented in figure 1. Tensile strength of fibres is given as 1100 MPa. Chopped basalt fibre of length 30 mm is used in concrete. Density is given as 2750 kg/m3 and tensile strength is given as 4840 MPa. Drinking water directly taken from water supply line was used for the entire casting work.

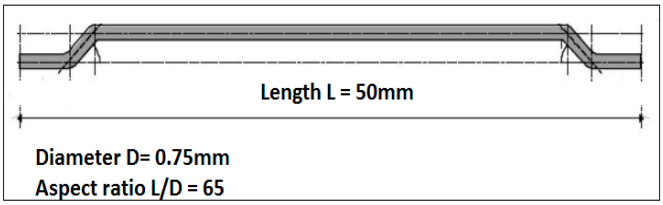

Fig 1:- Details of steel fibres

Fig 2:- Chopped basalt fibre (Borhan, 2013)

2.2 *Trial Mixes*

Three trial mixes were prepared with the proportion given in table 4. Compressive strength of standard cubes at 7, 14 and 28 days were determined as shown in table 5. The 28th day compressive strength of these mixes were examined and found that mix designated as M3 can be used for this study.

Mix No.	Weight of cement (kg/m^3)	Weight of coarse aggregate (kg/m^3)	Weight of fine aggregate (kg/m^3)	w/c	Mix proportion
M1	516.9	1186.1	595.27	0.3	1:1.15:2.3
M2	520	1140	685	0.3	1:1.31:2.2
M3	479.3	1150.5	642.9	0.3	1:1.34:2.4

Table 4:- Trial mix proportion

Mix No.	Compressive strength (MPa)		
	7 days	14 days	28 days
M1	47.2	60.3	65.77
M2	45.87	58.83	63.148
M3	51.3	61.7	68.3

Table 5:- Compressive strength of trial mixes

2.3 Casting and testing of cubes

Seventeen different mixes were prepared with varying percentage of steel and basalt fibres along with control mix. The size of the concrete cubes were 150 mm. The designation given to these mixes are shown in the table below.

Mix	Designation
Control mix	CL
0.5% steel	5S
1.0% steel	10S
1.5% steel	15S
2.0% steel	20S
2.5% steel	25S
0.1% basalt	1B
0.2% basalt	2B
0.3% basalt	3B
0.4% basalt	4B
0.5% basalt	5B
0.6% basalt	6B
1.8% steel+ 0.2% basalt	1SB
1.6% steel+ 0.4% basalt	2SB
1.4% steel+ 0.6% basalt	3SB
1.2% steel+ 0.8% basalt	4SB
1.0% steel+1.0% basalt	5SB

Table 6:- Specimen details

The cube moulds of required size 100 mm were made in so that the two parts get separated. Cube moulds were provided with a base plate and they were as per IS:10086-1982. The tamping rod was made of mild steel and its diameter was 16±0.5 mm and was of length 600±2 mm. the rod end was rounded for the ease of tamping. The compression testing machine was used for testing recommended by code. The compression testing machine was capable of applying the uniform load manually or automatically at the specified rate. Results showing compressive strength are shown in table 7.

Mix	28 days compressive strength (MPa)
CL	68.3
5S	69.7
10S	71.5
15S	**84.5**
20S	79
25S	66.8
1B	66.9
2B	71.2
3B	72.4
4B	**76.9**
5B	63.4
6B	61.4
1SB	47.5
2SB	57
3SB	63.8
4SB	**72**
5SB	48.2

Table 7:- 28 days Compressive strength of different mixes

From the above table it is clear that mixes 15S, 4B and 4SB are having the highest compressive strength as compared to the control mix and all other mixes. As the percentage of steel fibre increases the compressive strength is also increasing upto a percentage of 1.5% after which the compressive strength is decreasing. In case of basalt fibre the compressive strength is increasing upto 0.4%.For the mix having both steel and basalt fibres the compressive strength is higher for the combination 1.2% steel and 0.8% basalt. Hence it is clear that the optimum percentage of steel is 1.5% for steel fibre mix alone, basalt fibre is 0.4% for basalt fibre mix alone and the combined mix optimum percentage is 1.2% steel and 0.8% basalt. With this percentage keeping as constant beams were prepared.

2.4 Casting of Specimens

Rectangular plywood moulds of inner dimensions 100mmx150mmx1000mm were used. A rectangular cut of 3mm size was provided at the mid section so as to introduce a metallic template upto 30mm depth. 3mm metallic template is used to provide a sharp notch at the mid span of the specimen which can be removed after 5 hours of casting. Reinforced concrete beams with rectangular cross section of size 100 x150 mm and clear span of 1000mm were used to obtain fracture properties. Total of 8 beams were cast including control specimen, beams with 1.5% steel fibre, 0.4% basalt fibre and combination of 1.2% steel fibre and 0.8% basalt fibre. Designation of specimen is given in table 8.

Mix	Designation
Control Specimen	CL1
	CL2
1.5% steel fibre	BS1
	BS2
0.4% basalt fibre	BB1
	BB2
1.2% steel + 0.8% basalt fibres	SBB1
	SBB2

Table 8:- Specimen details

The beam consists of 3 bars of 10 mm diameter as tension steel. Two legged stirrups of 6 mm diameter were provided at 90 mm spacing at the end and 100 mm spacing at the centre. Two 8 mm diameter bars were provided as stirrup holders.

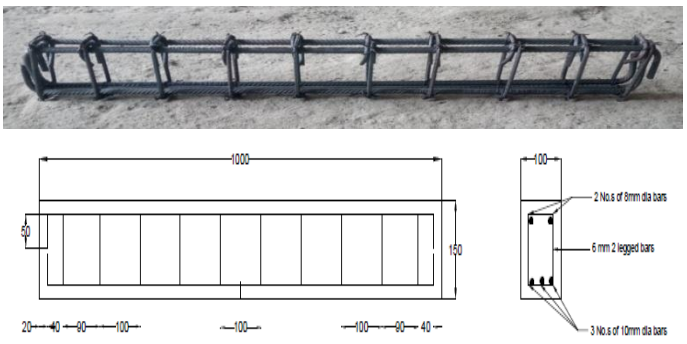

Fig 3:- Reinforcement Details (All dimensions in mm)

Materials were batched and weighed. Mixer was wetted before mixing to prevent absorption of water. First the coarse aggregate was mixed in mixer for 5 minutes. Later fine aggregate and cement were introduced in mixer and mixed for 5 minutes. Fibers were evenly distributed in

ISSN No:-2456-2165

the mixer. Water and admixtures were added to obtain a uniform paste.

Inner surface of mould was oiled and a 3 mm thick steel plate was inserted in the prescribed position in each wooden mould to produce a 30 mm deep initial crack. Reinforcement cage was placed in the mould and the whole assembly was kept elevated for removal of metal template. After 5 hours of casting the metal template was removed. Specimens were unmoulded (fig. 5) after 24 hours and cured for 28 days in water at room temperature.

Fig 4:- Reinforcement inserted in mould during casting

Fig 5:- Bottom surface of beam specimen with notch

2.5 Fracture test on specimens

Specimens were taken out from water, kept for drying and then white washed. Pellets and fixtures for LVDT were glued to specimens at the location to measure strain and CMOD respectively as shown in the schematic diagram of test set up in fig. 6. Load controlled testing were done by applying two point load. Mid-span deflection, CMOD were recorded at every 0.1 tone load increment. Beams were loaded till failure and ultimate load was noted.

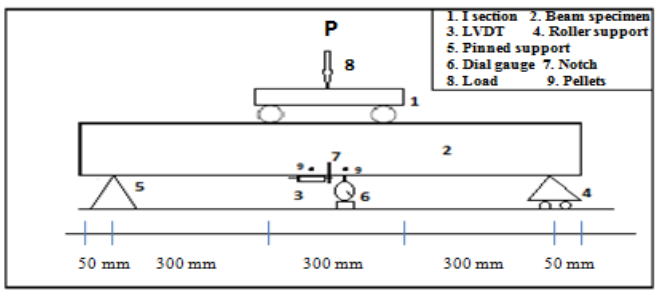

Fig 6:- Schematic diagram of test setup

III. RESULTS AND DISCUSSIONS

3.1 Initiation Load and Peak Load

Load corresponding to crack initiation is known as initiation crack. This can be obtained by monitoring stain at the level of tension steel. As the load increases the strain also increases and the energy will be stored in the specimen. At the crack initiation this energy is used for the formation of crack hence strain at that point decreases. Table 9 shows the initiation load of the specimens. Both steel and basalt fibre reinforced beam shows almost same results.

Specimen	P_{ini} (kN)	P_{un} (kN)	δ_{in} (mm)	δ_{un} (mm)
CL1	30	105	1.09	5.5
CL2	30	110	1.10	5.3
BS1	33	123	1.25	6.5
BS2	37	125	1.44	6.2
BB1	35	133	1.4	6.65
BB2	35	130	1.35	6.8
SBB1	34	95	0.65	5.9
SBB2	34	92	0.69	5.6

Table 9:- Initiation load and peak load of beams

Peak load is the maximum load carried by the beam specimens. Beams are loaded to failure and maximum load is recorded. Values of peak load for specimens are shown in table 9. Variation of peak load with specimen is shown in figure 8. Average peak load for specimen CL, BS, BB and SBB were obtained as 105 kN, 124 kN, 132 kN and 93.5 kN respectively.

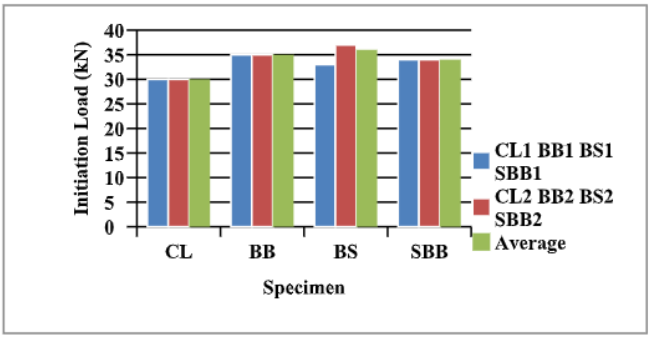

Fig 7:- Variation of initiation load with specimens

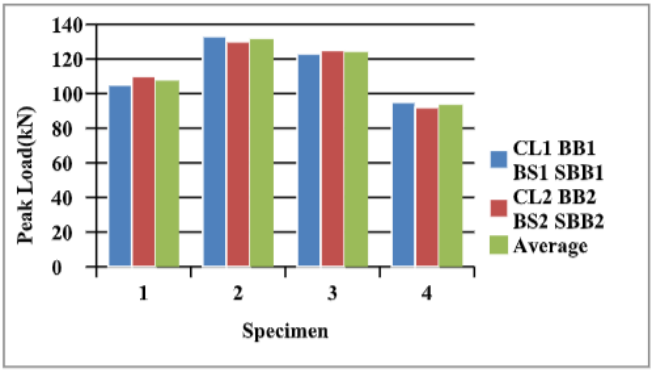

Fig 8:- Variation of peak load with specimens

3.2 Load deflection behaviour

Load deflection curve is one of the most important characteristic of specimens. With the help of load deflection curve fracture properties like fracture toughness, critical effective crack length can be obtained. Deflection of beam at mid-span is obtained by placing dial gauge around the notch. The values are obtained corresponding to every increment in load. Load deflection graph of each specimen is plotted in figure 9. The graph shows a linear pattern upto certain load and that load is the crack initiation load. After that point it shows a non linear variation indicating stable crack propagation. After some point the deflection just increases without increase in load, and that pattern is the unstable

crack propagation leading to failure. Specimen BB shows higher deflection.

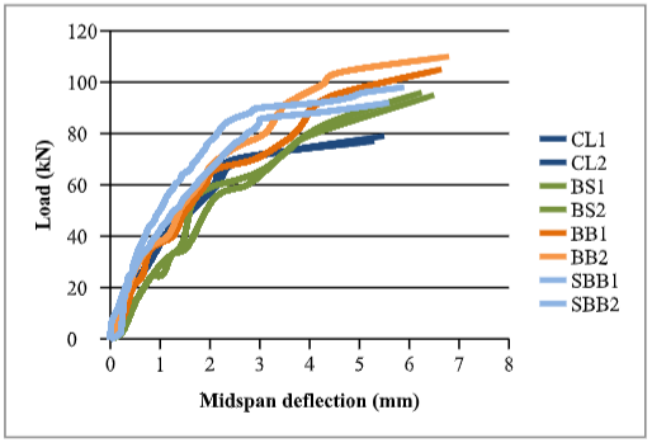

Fig 9:- Load – deflection curve

3.3 Load-CMOD behaviour

Crack mouth opening displacement (CMOD) is measured using LVDT placed at the bottom of beam. It is measured for each load increment and plotted in the graph shown in figure 10. CMOD increases linearly upto crack initiation point after which it shows a curved pattern during unstable crack propagation. CMOD for specimen SBB is higher.

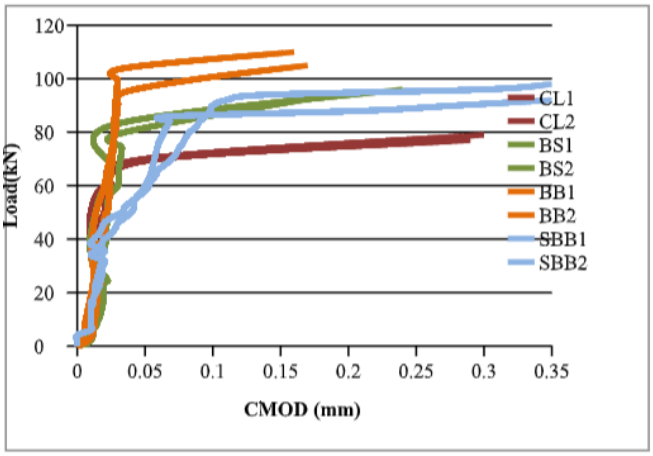

Fig 10:- Load-CMOD behavior

3.4 Fracture Energy

Fracture energy is calculated from area under load-deflection curve using equation 1.1. Results are tabulated in table 10.

$$G_f = \frac{W_F + W_S\delta_0}{A_{lig}} \qquad (1.1)$$

3.5 Intrinsic Brittleness

Intrinsic brittleness or in other words characteristic length of the specimens were obtained by substituting the values of modulus of elasticity and fracture energy in equation 1.2.

$$l_{ch} = \frac{EG_F}{f_t^2} \qquad (1.2)$$

Specimen	Fracture energy G_f (N/mm)	Young's Modulus (MPa)	Intrinsic brittleness (l_{ch}) (cm)
CL1	18.1	29307.2	658.3
CL2	17.04	29158.5	633.6
BS1	25.71	33537.5	872.3
BS2	25.03	32816.5	828.8
BB1	29.67	34191.7	1121.9
BB2	31.16	35418.5	110.3
SBB1	24.09	40840.0	1159.9
SBB2	21.467	38434.3	976.5

Table 10:- Fracture energy and intrinsic brittleness of beams

The average fracture energy for the beam specimens CL, BS, BB and SBB were obtained as 17.75 N/mm, 25.37 N/mm, 30.315 N/mm and 22.78 N/mm respectively.

Average values of intrinsic brittleness for specimens CL, BS, BB and SBB were 646 cm, 850.5 cm, 1166.1 cm and 1068.2 cm respectively.

3.6 Fracture Toughness

Fracture toughness of specimens was determined by set of equations from (1.3) to (1.7). Variation of fracture toughness with specimens is given in table 11. Fracture toughness was higher for specimen BB. The average value of fracture toughness was obtained as 1.373 MPa√m, 1.687 MPa√m, 2.537 MPa√m and 1.27 MPa√m respectively for specimens CL, BS, BB and SBB as shown in figure 11.

$$K_{IC} = K_{IC}^P - K_{IC}^S \qquad (1.3)$$

$$K_{IC}^P = \frac{6M\sqrt{a_0}}{BW^2}\,f(\alpha) \qquad (1.4)$$

f(α) is the geometric function for four point bending and is given in equation 1.5

$$f(\alpha) = 1.99 - 2.47\alpha + 12.97\alpha^2 - 23.17\alpha^3 + 24.8\alpha^4 + 60.5\alpha^{16}$$

$$\alpha = \frac{a_0}{h} \qquad (1.5)$$

$$K_{IC}^S = \frac{2F_S}{B\sqrt{\pi a_0}} F_1\left(\frac{c}{a_0}, \frac{a_0}{D}\right) \qquad (1.6)$$

$$F_1(\eta,\xi) = \frac{3.52(1-\eta)}{(1-\xi)^{\frac{3}{2}}} - \frac{4.35 - 5.28\eta}{\sqrt{1-\xi}} + \left[\frac{1.30 - 0.30\eta^{\frac{3}{2}}}{\sqrt{1-\eta^2}} + 0.83 + 1.76\eta\right](1-(1-\eta)\xi) \qquad (1.7)$$

ISSN No:-2456-2165

Specimen	Fracture toughness (MPa√m)	G_C (N/m)
CL1	1.388	65.7
CL2	1.366	63.9
BS1	1.718	88.63
BS2	1.656	83.56
BB1	2.744	219.57
BB2	2.33	153.26
SBB1	1.275	39.24
SBB2	1.281	42.68

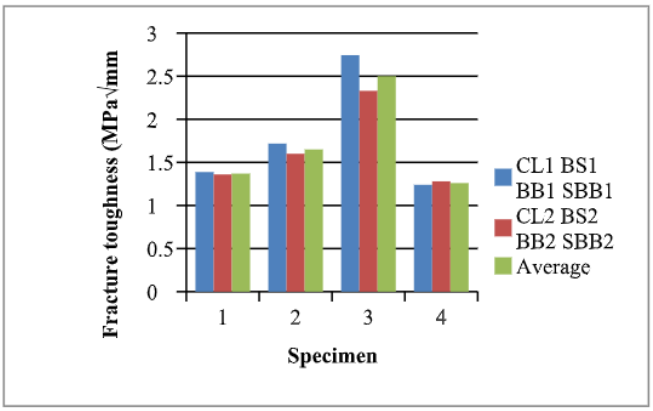

Fig 11:- Variation of fracture toughness with specimens

3.7 Critical Energy Release Rate

Critical energy release rate shows similar pattern as that of fracture toughness obtained from equation 1.8.

$$G_C = \frac{K_{IC}^2}{E} \qquad (1.8)$$

Average value of critical energy release rate was obtained as 64.8 N/m, 86.095 N/m, 186.41 N/m and 40.96 N/m respectively. The variation is shown in figure 12.

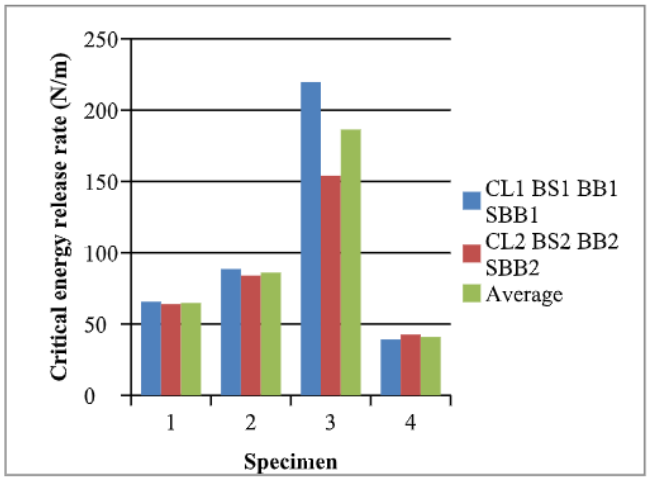

Fig 12:- Variation of critical energy release rate with specimens

3.8 Critical Effective Crack Length

Critical effective crack length was determined by substituting the value of maximum load and corresponding deflection in equation 1.9 and is shown in table 12.

$$E = \frac{P}{B\delta}\left(\frac{L}{W}\right)^3\left[\frac{23}{108}+\frac{5}{32}\frac{ql}{P}\right]+\frac{25(1+\mu)}{B\delta}\frac{L}{W}P\left(1+\frac{3ql}{P}\right)+\frac{3P}{B\delta}\left(1+\frac{3ql}{4P}\right)\left(\frac{L}{W}\right)^2 F(\alpha) \qquad (1.9)$$

Where, $F(\alpha) = \int_0^{a_0} x\left(Y(x)\right)^2 dx$

Specimen	Critical effective crack length (mm)
CL1	63.72
CL2	61.4
BS1	66.7
BS2	67.5
BB1	83.5
BB2	84.8
SBB1	68.53
SBB2	63.2

Table 12:- Critical effective crack length

The modulus of elasticity was determined by substituting values of load and corresponding deflection at crack initiation stage which was already determined and showed in table 10. Critical effective crack length for specimens CL, BS, BB and SBB were 62.56 mm, 67.1 mm 84.15 mm and 65.85 mm respectively.

3.9 Crack Pattern

Crack patter of beam specimens after testing is shown in figure 13. All the specimens were provided with initial crack at mid span which undergoes a growth during loading of beams.

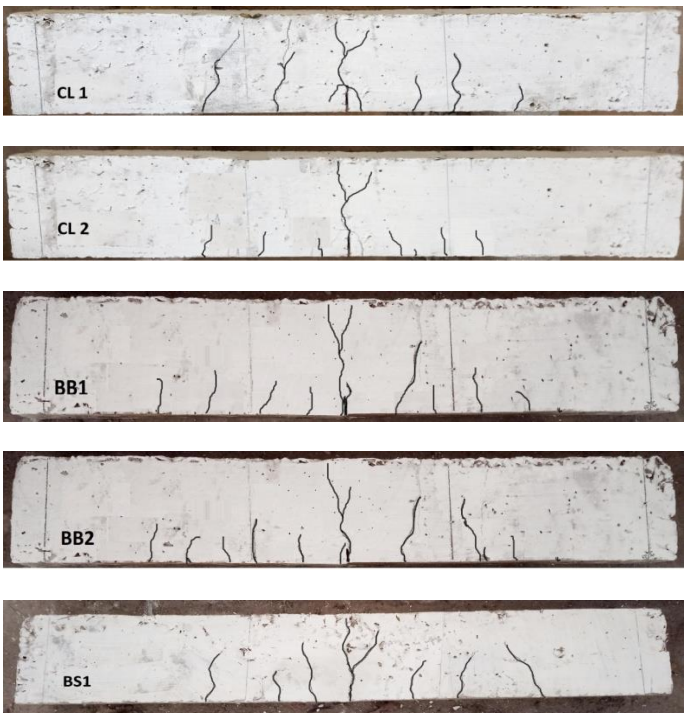

ISSN No:-2456-2165

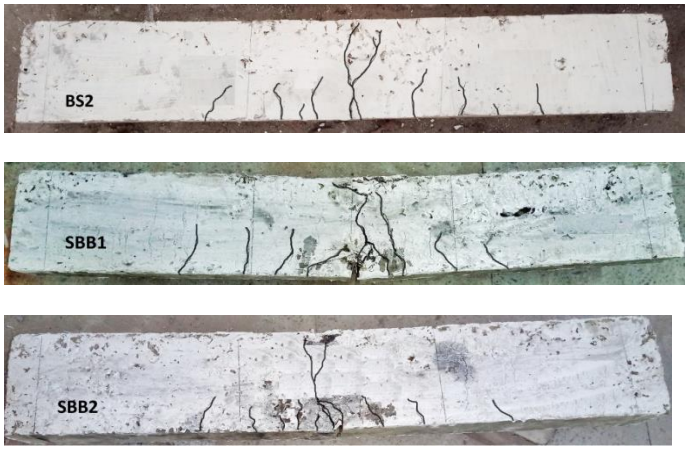

Fig 13:- Crack Pattern

IV. NUMERICAL PROGRAMME

4.1 Material Properties and Constitutive Models

Modeling of the beam was done for the dimensions similar to that of the specimens cast. Materials used for analysis includes concrete and steel reinforcement bars. Constitutive models for both steel reinforcement and concrete are available in the ABAQUS material library. Beam was modeled as a three dimensional solid continuum element (C2D8R) which can be called as a brick element or hexahedron and was used for analysis of behavior of fibre reinforced concrete. The elements consisted of eight nodes and each node has three degrees of freedom i.e., translations in x, y and z directions. For the modeling of steel reinforcing bars, a two dimensional truss element was used (T3D2) with two nodes. Each node has three degrees of freedom same as that of the beam element. The properties given for steel reinforcing bars include an average value of yield stress of 500 MPa, Young's Modulus of 210 GPa and Poisson's ratio of 0.3. The properties of concrete input were Young's modulus of 2000 MPa for plain concrete and for other beam models this value varied. The compressive strength, tensile strength and Poisson's ratio varies with each beam model.

4.2 Details of Beam Specimen

Reinforced concrete beams with rectangular cross section of size 100 mm width, 150 mm depth, 1000mm length were modeled using ABAQUS software. The beam consists of 3, 10 mm diameter bars as tension steel. Two legged stirrups of 6 mm diameter were provided at 100 mm spacing at the end and 90 mm spacing at the centre. Two 8 mm diameter bars were provided as stirrup holders.

4.3 Boundary and Loading Conditions

The boundary conditions for the reinforced concrete beams considered were simply supported with one end hinged and other end roller. For hinged support, since there is no movement in any directions, all the three displacements along x, y, and z directions are arrested i.e., U1 = U2 = U3 = 0. In case of roller support, it can be moved in only one direction i.e., along x direction so U1 ≠ 0 while the other two displacements along y and z directions are arrested (U2 = U3 = 0). The modeled beam with both types of boundary conditions is shown in Fig. 14. Here, the beam is analyzed under four point loading condition. So the load applied is distributed at one third point on beam and acts as a uniform pressure along that line.

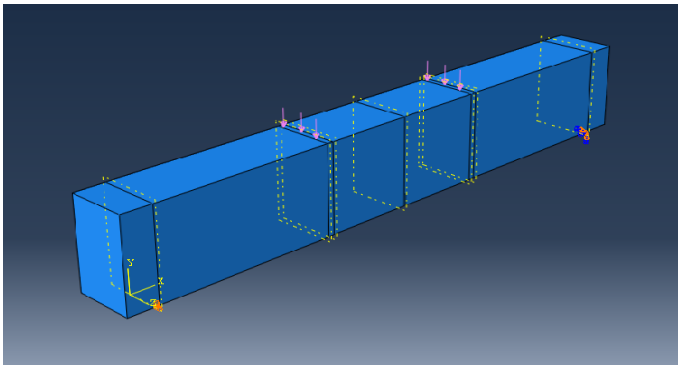
Fig 14:- Beam model with loading and boundary conditions

4.4 Interactions

In modeling part, both the concrete beam element and steel reinforcing bar element are created separately and the properties are also assigned separately. So these act as two different elements. It is important for these to act as a single element. For this these have to act as a whole assembly. Hence, for this these to act as a whole assembly which can be attained by a tool called "Interactions" in ABAQUS. Since the steel is inserted into the concrete it is assumed to be embedded fully into the concrete mass, hence "Embedded Region" interaction is given to provide necessary contact between them. The interaction given between reinforcement and concrete is shown in Fig. 15.

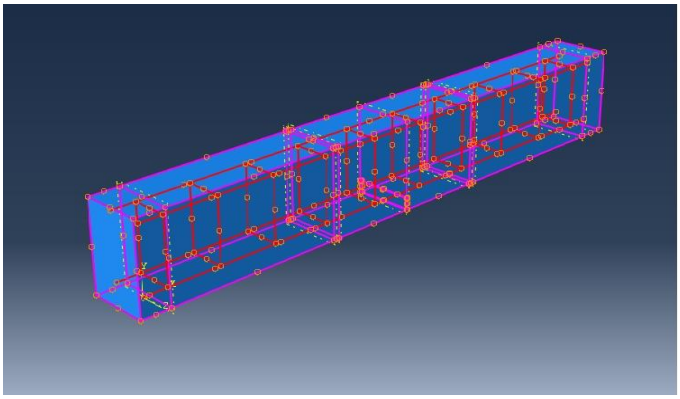
Fig 15:- Interaction between concrete and steel reinforcement

4.5 The Finite Element Mesh

All the elements of finite element model were assigned the same mesh size. This was done so that the two different materials can share the same node among them and to attain a good accuracy. Total number of nodes used were 12678. The mesh type selected in the model is given in figure 16. The mesh element for concrete assigned was 3D solid element and for steel bars 2D truss element is assigned.

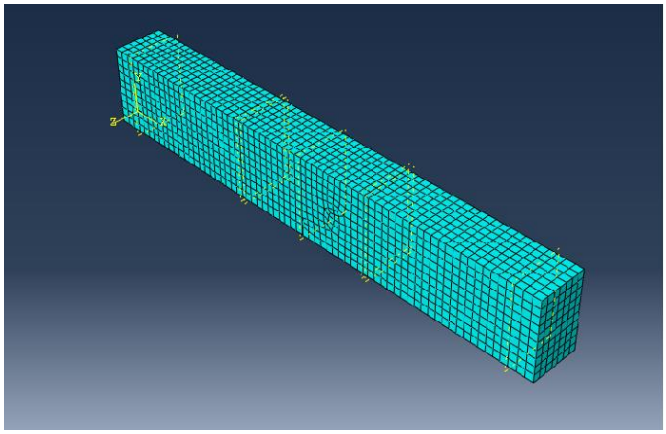

Fig 16:- Finite Element meshed Model in ABAQUS

V. RESULTS AND DISCUSSIONS

5.1 Comparison of results

5.1.1 Load deflection curve at mid span

The deflection was measured in the middle of the span at the bottom face of the beam. Figure 17 shows the load deflection curve of the 0.4 % basalt fibre reinforced beam and figure 18 shows the load deflection for 1.5% steel fibre reinforced beam for both finite element analysis and experimental data. The results from the finite element correlate well with those from the experimental data.

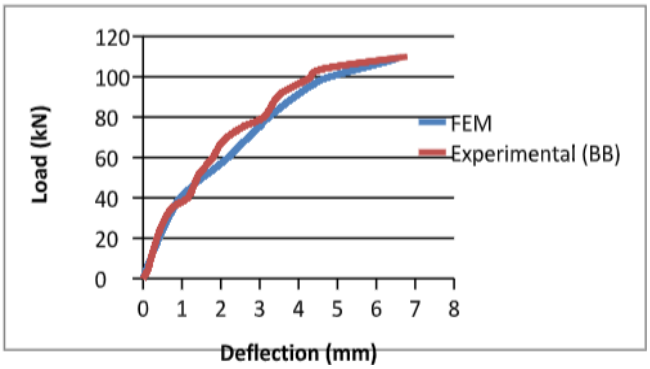

Fig 17:- Load – deflection curve for 0.4% basalt fibre beam

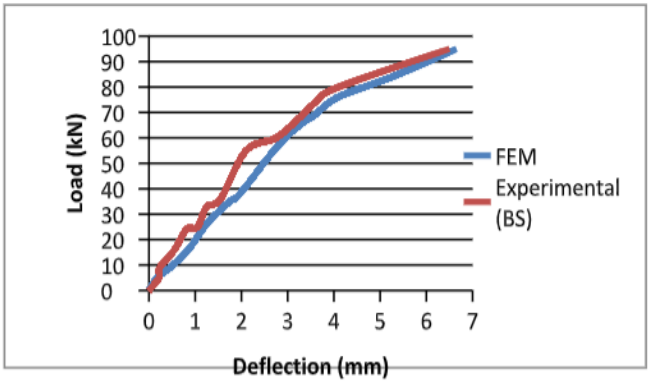

Fig 18:- Load – deflection curve for 1.5% steel fibre beam

5.1.2 Fracture Energy and Critical Effective Crack Length

Properties	Basalt			Steel		
	Exp.	FEM	Error %	Exp.	FEM	Error %
δ_{un} (mm)	6.75	6.55	2.96	6.375	6.65	4.313
Fracture energy G_f (N/mm)	30.41	30.02	1.28	25.32	26.3	3.8
Critical effective crack length (mm)	84.15	91.86	9.16	67.1	60	10.5

Table 13:- Comparison of fracture properties

The fracture energy is calculated based on the area under the load deflection curve obtained from ABAQUS. Based on fracture energy, effective crack length is obtained using relevant equation. Table 13 shows the values of fracture properties for both FEM and experimental data.

5.2 Numerical results of other volumes

5.2.1 Basalt fibre concrete

Basalt fibre reinforced concrete with other fibre volumes were used for numerical study. Specimens were designated as 1B (0.1%), 2B (0.2%), 3B (0.3%) and 5B (0.5%). The load deflection curve for the specimens is shown in figure 19.

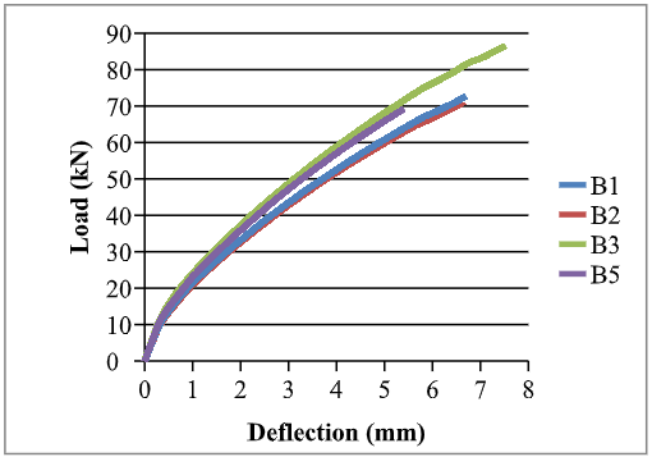

Fig 19:- Load – deflection curve for various volumes of basalt fibre

Based on the load deflection curve fracture energy and critical effective crack length was obtained. Table 14 depicts the ultimate load and corresponding deflection and fracture properties for various volumes of basalt fibre.

Specimen	P_{un} (kN)	δ_{un} (mm)	G_f (N/mm)	Critical effective crack length (mm)
1B	**79**	**6.5**	**21.39**	**74.38**
2B	**80**	**6.69**	**22.23**	**76.86**
3B	**86**	**7.51**	**26.9**	**79.6**
5B	**69**	**5.39**	**15.49**	**68.29**

Table 14:- Fracture properties of basalt fibre concrete beams

Among the four mixes mentioned above, 3B having 0.3% of basalt fibre posses higher fracture energy. It means that higher energy is required for specimen 3B to open the crack that is it can withstand more crack opening. It is clear that as the percentage of basalt fibre increases the fracture energy also increases upto 0.3% of basalt fibre. Similarly specimen 3B is having higher effective crack length.

5.2.2 Steel fibre concrete

Steel fibre reinforced concrete with other fibre volumes were used for study. Specimens were designated as 5S (0.5%), 10S (1.0%), 20S (2.0%) and 25S (2.5%). The load deflection curve for the specimens is shown in figure 20.

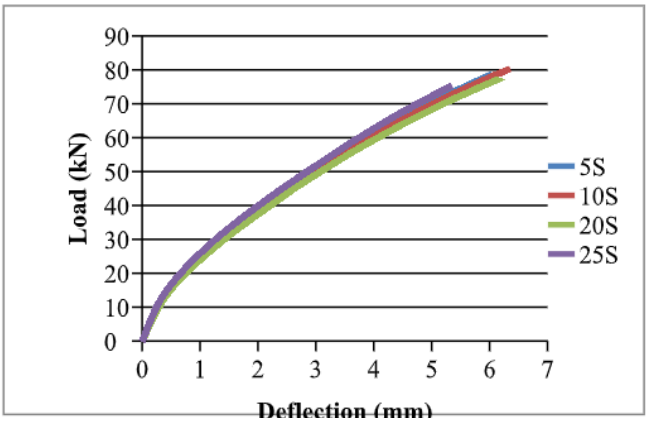

Fig 20:- Load – deflection curve for various volumes of steel fibre

Based on the load deflection curve fracture energy and critical effective crack length was obtained. Table 15 depicts the ultimate load and corresponding deflection and fracture properties for various volumes of steel fibre.

Specimen	P_{un} (kN)	δ_{un} (mm)	G_f (N/mm)	Critical effective crack length (mm)
5S	**78.7**	**6.04**	**19.8**	**71.24**
10S	**80.32**	**6.3**	**21.08**	**72.5**
20S	**77.2**	**6.14**	**19.75**	**70.05**
25S	**76**	**5.34**	**16.91**	**66.9**

Table 15:- Fracture properties of steel fibre concrete beams

Among the four mixes, 10S having 1% of steel fibre posses higher fracture energy of 21.08 N/mm as well as higher effective crack length of 72.5 mm.

VI. CONCLUSIONS

From the study conducted following conclusions can be drawn.

1) The initiation load of basalt fibre beams were higher as compared to conventional reinforced concrete (RC) beams and steel fibre beams. This may be due to the fine structure of basalt fibre that creates a better bridging property than steel fibre that prevents initiation of crack.
2) Ultimate load of beams with 0.4% basalt fibre was obtained as 133 kN and that of 1.5% steel fibre was obtained as 125 kN. Beams with combination of 1.2% steel fibre and 0.8% basalt fibre had a peak load of 95 kN.
3) Fracture energy of beams with 0.4% basalt fibre was 71.45% higher than conventional RC beams. Fracture energy of beams with 1.5% steel fibre and beams with combination of 1.2% steel fibre and 0.8% basalt fibre were 45% and 31.4% higher respectively as compared to conventional RC beams.
4) Fracture toughness of beams having 0.4% basalt fibre and beams having 1.5% steel fibre were 85% and 24.4% higher respectively as compared to conventional RC beams. Beams with combination of 1.2% steel and 0.8% basalt fibre had fracture toughness 8% higher than conventional RC beams.
5) Energy release rate of beams with 0.4% basalt fibre, beams with 1.5% steel fibre and beams with combination of 1.2% steel fibre and 0.8% basalt fibre were 191.8%, 32.8% and 12.5% higher respectively as compared to conventional RC beams.
6) Intrinsic brittleness of beams having 0.4% basalt fibre, beams having 1.5% steel fibre and beams with combination of 1.2% steel fibre and 0.8% basalt fibre

increased by 79.68%, 32.8% and 56% respectively as compared to conventional RC beams.

7) Critical effective crack length of beams having 0.4% basalt fibre, beams having 1.5% steel fibre and beams with a combination of 1.2% steel and 0.8% basalt fibre increased by 35.4%, 8.06% and 4.8% respectively as compared to conventional RC beams.
8) The experimental values of beams with 0.4% basalt fibre and 1.5% steel fibre content were used to validate the numerical values obtained from ABAQUS software which showed a good correlation with a percentage error of less than 10%.
9) Other mixes which are beams having 0.1, 0.2, 0.3, 0.5% basalt fibre content and beams having 0.5, 1.0, 2.0, 2.5% steel fibre content were considered for numerical study. The load-deflection curves for these mixes were obtained. All the mixes showed a similar pattern of curve but their effect on peak load were different.
10) Among the mixes, beams with 0.3% basalt fibre content and beams with 1% steel fibre content had higher peak load which is 86 kN and 80.32 kN respectively.
11) Also the fracture energy of beams with 0.3% basalt fibre content and 1% steel fibre content was higher with 26.9 N/mm and 21.08 N/mm.
12) Critical effective crack length for the specimen were 79.6 mm and 72.5 mm respectively.
13) It can be concluded that beams with basalt fibre content had better fracture properties than beams with steel fibre content.
14) The results of fracture energy, fracture toughness and energy release rate of beams with optimum of 0.4% basalt fibre content, demonstrated that it acquired better ductile behavior and energy absorption capacity compared to all other mixes as well as ordinary concrete specimens.

REFERENCES

[1]. Anderson, T.L. Fracture Mechanics Fundamentals and Applications, Third Edition, Taylor and Francis, Boca Raton, 2010.
[2]. Aravind, R and Athira Das (2017) Experimental Investigation on the Fracture Behavior of Steel Fiber Reinforced Concrete, IRJET, 04, 2346-2355
[3]. Bencardino, F., L. Rizzuti, G. Spadea and R. N. Swamy (2010) Experimental evaluation of fiber reinforced concrete fracture properties, Composite Part B, 41, 17-24.
[4]. Chen, G. M, H. Yang, C. J. Lin, J. F. Chen, Y. H. He and H. Z. Zhang (2016) Fracture Behavior of Steel Fibre Reinforced Recycled Aggregate Concrete After Exposed to Elevated Temperature, Construction and Building Materials, 128, 272-286.
[5]. Fathima, I. I. A (2014) Strength Aspects of Basalt Fiber Reinforced Concrete, IJIRAE, 01, 192-198.
[6]. Guo, Y. C, J. H. Zhang, G. Chen, G. M. Chen and Z. H. Xie (2014) Fracture Behaviors of a New Steel Fibre Reinforced Recycled Aggregate Concrete with Crumb Rubber, Construction and Building Materials, 53, 32-39.
[7]. IS: 456-2000. Plain and Reinforced Concrete-Code of Practice, 4th Revision, BIS, New Delhi.
[8]. Kizilkanat, A. B, N. Kabay, V. Akyüncü, S. Chowdhury and A. H. Akça (2015) Mechanical Properties and Fracture Behavior of Basalt and Glass Fiber Reinforced Concrete: An Experimental Study, Construction and Building Materials, 100, 218-224.
[9]. Krishna, K. M and Ganesh Naidu Gopu (2016) Analysis of Fracture Parameters in Concrete by using ABAQUS Software, IJSER, 03, 108-113.
[10]. Kumar, M. V, K. Niveditha, B. Anusha and Bontha Sudhakar (2017) Comparison Study of Basalt Fibre and Steel Fibre as Additives to Concrete, IJRASET, 05, 6-14
[11]. Long, N. M and R. Marian (2007) Investigation of Fracture Properties of Steel Fiber Reinforced Concrete, Material Science and Engineering, 96, 854-861.
[12]. Martin, J., J. Stanton, N. Mitra, and L. N. Lowes (2007) Experimental Testing to Determine Concrete Fracture Energy Using Simple Laboratory Test Setup, Material Journal, ACI, 104(6), 575-584.
[13]. Ruiz, G., M. Elices and G. Planas (1998) Experimental Study of Fracture of Lightly Reinforced Concrete Beams, Material and Structures, 31, 683-691.
[14]. Tong, L., Bo Liu and Xiao-Ling Zhao (2017) Numerical Study of Fatigue Behavior of Steel Reinforced Concrete (SRC) Beams, Engineering Fracture Mechanics, 178, 477-496
[15]. Tumadhir, M and Borhan (2013) Thermal and Mechanical Properties of Basalt Fibre Reinforced Concrete, World Academy of Science, Engineering and Technology, 04, 334-337.
[16]. Vikranth, S. V, and S. K. Kavitha (2012) Introduction to Properties of Steel Fibre Reinforced Concrete on Engineering Performance of the Concrete, International Journal of Science and Technology Research, 1(4), 139-141.
[17]. Yamini, R. S, P. Magudeaswaran, D. S. Marvel and P. Eswaramoorthi (2016) Analytical Study on Flexural Behavior of Concrete Beams Reinforced with Steel Rebars by ABAQUS, IJRIET, 02, 35-39.